Anthropogenic aerosols influence tropical Pacific Sea surface temperature gradient trends

Maher, P. ORCID: https://orcid.org/0000-0001-8513-8700, Chadwick, R. ORCID: https://orcid.org/0000-0001-6767-5414, Collins, M. ORCID: https://orcid.org/0000-0003-3785-6008, Booth, B. B. B. ORCID: https://orcid.org/0000-0002-0715-2141 and Dittus, A. ORCID: https://orcid.org/0000-0001-9598-6869
(2026) Anthropogenic aerosols influence tropical Pacific Sea surface temperature gradient trends. Geophysical Research Letters, 53 (11). e2025GL121248. ISSN 0094-8276 doi: 10.1029/2025GL121248 Available at https://centaur.reading.ac.uk/130618/

Geophysical Research Letters

RESEARCH LETTER
10.1029/2025GL121248

Anthropogenic Aerosols Influence Tropical Pacific Sea Surface Temperature Gradient Trends

Penelope Maher[1], Robin Chadwick[1,2], Matthew Collins[1], Ben B. B. Booth[2], and Andrea Dittus[3]

[1]Department of Mathematics and Statistics, University of Exeter, Exeter, UK, [2]Met Office Hadley Centre, Met Office, Exeter, UK, [3]National Centre for Atmospheric Science and Department of Meteorology, University of Reading, Reading, UK

Key Points:

- Historical CMIP6 tropical Pacific gradient trends are primarily a balance between responses to anthropogenic aerosols and greenhouse gases
- The effective radiative forcing of anthropogenic aerosols can not account for the inter-model differences in the gradient trend
- All models predict future weakening of the tropical Pacific gradient, irrespective of their historical response

Supporting Information:

Supporting Information may be found in the online version of this article.

Correspondence to:

P. Maher,
p.maher@exeter.ac.uk

Citation:

Maher, P., Chadwick, R., Collins, M., Booth, B. B. B., & Dittus, A. (2026). Anthropogenic aerosols influence tropical pacific sea surface temperature gradient trends. *Geophysical Research Letters*, *53*, e2025GL121248. https://doi.org/10.1029/2025GL121248

Received 15 DEC 2025
Accepted 12 MAY 2026

Author Contributions:

Conceptualization: Penelope Maher, Robin Chadwick, Matthew Collins
Formal analysis: Penelope Maher, Robin Chadwick, Matthew Collins
Funding acquisition: Robin Chadwick, Matthew Collins
Investigation: Penelope Maher, Ben B. B. Booth, Andrea Dittus
Methodology: Penelope Maher, Robin Chadwick, Matthew Collins, Andrea Dittus
Project administration: Robin Chadwick
Software: Penelope Maher
Validation: Penelope Maher

Abstract The tropical Pacific is warming more in the west than the east. This observed strengthening of the tropical Pacific east-to-west Sea Surface Temperature (SST) gradient is poorly reproduced in climate models—a prominent model bias with far reaching global impacts. We explore the tropical Pacific SST gradient response to anthropogenic aerosols in large-ensembles of CMIP6 simulations between 1950 and 2014. We find that anthropogenic aerosols are cooling the tropical Pacific—the cooling is more pronounced in the east Pacific—while greenhouse gases have the opposite response. Tropical Pacific gradient strengthening is not due to the anthropogenic aerosol effective radiative forcing magnitude or top of atmosphere energy imbalance. This suggests that pathways connecting the regional radiative response to the tropical Pacific are important. In the future, all models predict a weakening gradient, irrespective of historical trends. Anthropogenic aerosol forcing plays an important role in driving changes in tropical Pacific SSTs.

Plain Language Summary The tropical Pacific is the single most important driver of global climate, evident during El Niño-Southern Oscillation events which impact weather and climate in all regions. The equatorial Pacific SST pattern is dominated by a warm pool in the west and cold tongue in the east. This east-to-west SST gradient has strengthened over the last half century—the west Pacific is warming more than the east. The origins of this strengthening remains illusive, despite many proposed mechanisms. Climate models struggle to capture the observed strengthening of the tropical Pacific gradient trend. In historical simulations, the gradient trends are primarily a balance between anthropogenic aerosols that strengthen the trend and greenhouse gas forcing that weaken the trend. The radiative impact of anthropogenic aerosols can't explain the response of the tropical Pacific in the models, suggesting the processes that connect regional forcing to the tropical Pacific response are important. Each model predicts future weakening of the tropical Pacific gradient, irrespective of their response in historical simulations.

1. Introduction: The Discrepancy Between Observed and Modeled Tropical Pacific SST Gradient

The response of the tropical Pacific to climate change is of profound importance for predicting future climate because of its strong influence on atmospheric and ocean circulation, rainfall and temperature patterns, climate sensitivity and tropical cyclones (Andrews et al., 2018; Good et al., 2021; Lin & Qian, 2019; Lee et al., 2022; Sobel et al., 2023; Ying et al., 2022). The global importance of the tropical Pacific is evident during El Niño-Southern Oscillation (ENSO) events associated with variability in the east-to-west sea surface temperature (SST) gradient. Observed SST trends show warming in the western tropical Pacific while the central and eastern tropical Pacific have less pronounced warming or even cooling, depending on the time period.

The community is debating the mechanisms for the observed tropical Pacific gradient strengthening (Lee et al., 2022; Watanabe et al., 2024) and the role that greenhouse gases (Seager et al., 2019) and anthropogenic aerosols (Heede & Fedorov, 2021; Hwang et al., 2024; Kuo et al., 2023; Verma et al., 2019) play in shaping the tropical Pacific SST response. Some of the proposed mechanisms include the ocean thermostat (Clement et al., 1996; Heede et al., 2020), cloud feedbacks (Clement et al., 2009; Ying et al., 2016), land-sea heating contrast (Günther et al., 2025), and the role of subsurface cooling (Jiang et al., 2025). The variety of mechanisms highlights the complex nature of the coupling between the ocean and atmosphere.

Visualization: Penelope Maher
Writing – original draft: Penelope Maher
Writing – review & editing: Penelope Maher, Robin Chadwick, Matthew Collins, Ben B. B. Booth, Andrea Dittus

Attributing the origins of the observed strengthening trend is further complicated by multi-decadal natural variability. The Pacific Decadal Oscillation (PDO) and decadal variability of ENSO are the primary sources of natural variability that impact tropical Pacific SST trends. Fluctuations in the PDO alone do not explain the observed trends (Heede & Fedorov, 2023; Wills et al., 2022) and there is growing evidence to suggest the east Pacific cooling is a forced response (Coats & Karnauskas, 2017; Heede & Fedorov, 2023; Luongo et al., 2023; Seager et al., 2019; Watanabe et al., 2021). Jiang et al. (2024) proposed that the tropical Pacific forced SST response is a narrow band of cooling in the eastern equatorial Pacific SSTs and warming elsewhere.

Climate models generally fail to capture the magnitude of the observed strengthening in the SST gradient and many models have the wrong sign of the trend, that is, a weakening of the SST gradient (Byrne et al., 2025; Jiang et al., 2025; Olonscheck et al., 2020; Watanabe et al., 2021; Wills et al., 2022). Models which capture the strengthening of the tropical Pacific gradient may not reproduce the observed behavior for the correct reasons. For example, Byrne et al. (2025) recently showed that CMIP6 model strengthening is associated with excessive internal variability and the forced response is a weakening of the gradient trend.

There are many plausible explanations for the discrepancy in tropical Pacific SST trends between observations and CMIP6 historical simulations. These include: climate model mean-state biases, missing key processes, underestimating the internal variability and not capturing the forced response (Heede & Fedorov, 2023; Hwang et al., 2024; Lee et al., 2022; Rugenstein et al., 2023; Seager et al., 2019; Wills et al., 2022). Pervasive model biases include the cold tongue bias which is linked to a weaker tropical Pacific SST gradient (Li et al., 2016; Dhame et al., 2025), the double Intertropical Convergence Zone (ITCZ) bias which may block teleconnections (Hwang et al., 2024), the surface zonal wind stress (Li et al., 2020) and thermocline structure bias (Dhame et al., 2025). Model resolution is also important for representing trends in the east Pacific but higher resolution alone does not bring CMIP6 models into agreement with observed trends (Dhame et al., 2025). The problem is further complicated by the time dependence of the trend, where the strength of the trend depends on the time period (Byrne et al., 2025; Olonscheck et al., 2020).

Idealized model studies that abruptly add or remove anthropogenic aerosols have been pivotal for understanding how their emissions impact the climate. Enhanced cooling in the Northern Hemisphere due to anthropogenic aerosols emissions creates an energy imbalance with the Southern Hemisphere. The atmosphere redistributes the energy imbalance by shifting the Hadley circulation southward (Verma et al., 2019), following the energetics framework (Kang et al., 2018), resulting in a southward shift of the ITCZ. This shift intensifies the trade winds, resulting in coastal Ekman upwelling, and low cloud wind-evaporation-SST (WES) feedback (Hwang et al., 2024). The ocean also responds on longer timescales, where the subtropical cell strengthens and cools the east Pacific SSTs (Hwang et al., 2024). These idealized studies have shown that La-Niña-like surface warming results from the combined atmosphere and ocean responses to anthropogenic aerosols.

These idealized studies motivate this work as they have shaped our understanding of how anthropogenic aerosols impact tropical Pacific SSTs. Our research question is: *Do anthropogenic aerosols impact historical tropical Pacific SST gradient trends?* To answer this research question we first explore the tropical Pacific SST trends in observations and large-ensembles of historical simulations. Large-ensemble simulations are ideal for understanding the forced response of the tropical Pacific as they capture the range of possible internal variability within the models. We then use the single-forcing CMIP6 simulations to explore how anthropogenic aerosols (AA), greenhouse gases (GHG), and tropospheric and stratospheric ozone (O_3) contribute to the historical tropical Pacific SST trends.

2. Data and Methods

2.1. Observational Data Sets

Three monthly SST observational data sets are used for 1950–2014. First, the National Oceanic and Atmospheric Administration Extended Reconstructed SST V5 (ERSST5) data set. Second, the COBE-SST2 SST and Ice data set. Finally, the Met Office Hadley Center sea ice and SST data set version 2 (HadISST.2.1.0.0), which is a 10 member ensemble data set available until 2010. Each realization is generated by using different bias adjustments to the data. See Table 1 for data and model citations and Table S1 in Supporting Information S1 for resolution and ensemble size.

Table 1
CMIP6 Models (LESFMIP Models in Bold) and Observations Used in This Study, Their Citation and Data Citation

Model or observations	Model citation	Data citation
ACCESS-ESM1-5	Ziehn et al. (2020)	Ziehn et al. (2019)
CanESM5	Swart et al. (2019a)	Swart et al. (2019b)
CNRM-CM6-1	Voldoire et al. (2019)	Voldoire (2018)
EC-Earth3	Döscher et al. (2022)	EC-Earth Consortium (2019)
GISS-E2-1-G	Kelley et al. (2020)	NASA-GISS (2018)
HadGEM3-GC31-LL	Kuhlbrodt et al. (2018)	Ridley et al. (2019)
IPSL-CM6A-LR	Boucher et al. (2020)	Boucher et al. (2018)
MIROC6	Tatebe et al. (2019)	Tatebe and Watanabe (2018)
MPI-ESM1-2-LR	Mauritsen et al. (2019)	Wieners et al. (2019)
NorCPM1	Bethke et al. (2021)	Bethke et al. (2019)
UKESM1-0-LL (MOHC)	Sellar et al. (2019)	Tang et al. (2019)
UKESM1-0-LL (NIMS-KMA)	Sung et al. (2021)	Byun (2020)
ERSST5	Huang et al. (2017a)	Huang et al. (2017b)
COBE-SST2	Hirahara et al. (2014)	PSL (2023)
HadISST.2.1.0.0	Titchner and Rayner (2014)	Rayner et al. (2003); MOHC (2024)

2.2. Historical and Large Ensemble Model Data

CMIP6 large ensembles with monthly historical surface temperature (*ts*) data are considered for models with 15 or more members. Only large ensembles are considered in order to sample the internal variability of each model. CMIP6 models which contributed at least 15 realizations to the Large Ensemble Single Forcing Model Intercomparison Project (LESFMIP) (Smith et al., 2022) are examined further. These single forcing experiments are piControl simulations in which one historical forcing is applied. These forcing agents include: natural forcing from solar radiation and volcanic eruptions (*hist-nat*), historical well-mixed greenhouse gases (*hist-GHG*), historical anthropogenic aerosol (*hist-aer*) and historical ozone (*hist-totalO3*). See Milinski et al. (2020) for a discussion on the importance of ensemble size and the LESFMIP protocol paper Smith et al. (2022) for details of the experiments. CMIP6 and LESFMIP models are listed in Table 1, and their resolution and ensemble sizes in Tables S1 and S2 of Supporting Information S1. Only 47 of the 55 available HadGEM3-GC3.1-LL members are used, as only 52 members have unique branching dates and the last five realizations have unrealistic warming trends beyond 2030 in the piControl simulations (Mutton et al., 2024; Ridley et al., 2022). The GISS-E2-1-G model is treated as three separate models following Smith et al. (2020) as there are three physics variants: *p1* has non-interactive aerosols and ozone, *p3* a one-moment prognostic aerosols and ozone scheme, and *p5* a quadrature moment scheme (Miller et al., 2021). CanESM5 only have 10 realizations for *hist-totalO3*, however, we included the model in this analysis as the other single-forcing experiments have 30 realizations each.

2.3. East-To-West (E:W) Index Trend

The annual east-to-west (E:W) index is defined as: east Pacific SST (5°S–5°N, 180°–80°W) minus west Pacific SST (5°S–5°N, 110°E – 180°) following Watanabe et al. (2021). The *ts* data is masked to exclude land. The E:W trend is the least squares linear regression for the 1950–2014 period and multiplied by 100 for "K per century" trends. We focus on the forced trends in the historical period. We use the 1950–2014 period to maximize the decadal variability included in the time series, without compromising on data quality prior to 1950 or losing the signal in the trend over a longer time periods.

3. Results and Discussion

3.1. Observed and Historical CMIP6 Model Tropical Pacific SST Gradient Trends

To provide motivation for the analysis of single-forcing model trends, we first consider observed and modeled historical tropical Pacific east-to-west SST gradient trends between 1950 and 2014. The observed trends range

10.1029/2025GL121248

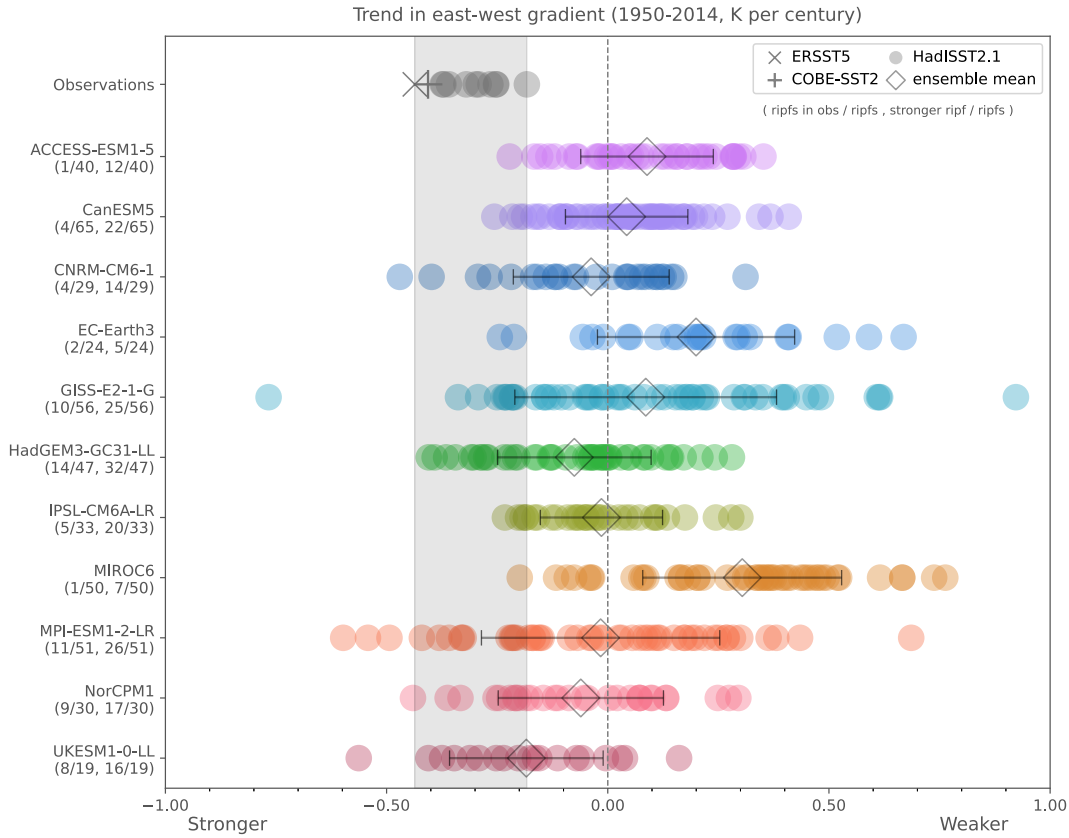

Figure 1. Observed and CMIP6 large-ensemble east-to-west gradient trends of surface temperature (K per century) for the period 1950–2014, except HadISST.2.1.0.0 which is 1950–2010. Negative trends correspond to a strengthen trend (east Pacific cooling or west Pacific warming) and visa versa. Observations in gray include ERSST5 ("x"), COBE-SST2 ("+") and the 10 member HadISST.2.1.0.0 ("O") data sets. The observational trend range is −0.436 to −0.183 (gray column). The ensemble-mean of each model is "⋄". The $\pm 1\sigma$ range is shown for each model. Under the title of each model is the number of ensemble members that are within the range of the observations (i.e., lies within the gray column) per ensemble size and the number of realizations that have a strengthening trend (i.e., a negative trend) per ensemble size.

from −0.436 to −0.183 K per century for the three observational data sets, see Figure 1. These trend values are consistent with the literature, see Table S3 in Supporting Information S1.

To capture both the internal variability and forced response in the tropical Pacific, we consider historical CMIP6 simulations with large ensembles. Of the 11 CMIP6 large-ensemble models in Figure 1, six have ensemble-mean trends that strengthen like observations while five weaken. The spread in the ensemble-means between different models is consistent with the literature (Jiang et al., 2025; Olonscheck et al., 2020; Simpson et al., 2025; Watanabe et al., 2021; Wills et al., 2022). The one-sigma range straddles the zero trend line for most models, except MIROC6 with the largest weakening and UKESM1-0-LL the largest strengthening ensemble-means, 0.30 and −0.18 K per century respectively. UKESM1-0-LL is the only model to have an ensemble-mean that lies in the range of observations.

The observed gradient trends are sensitive to the trend period (Byrne et al., 2025; Olonscheck et al., 2020), as different time periods sample different features of the natural variability and the forced response. During the 1979–2014 period the observed trends are four times larger, however, the models have similar ensemble-mean trends, see Figure S1 in Supporting Information S1. As such, the discrepancy between models and observations are amplified in the 1979–2014 period. While UKESM1-0-LL has the largest ensemble-mean strengthening trend in the 1950–2014 period, it has a near-zero trend in the shorter 1979–2014 period. See Supporting Information S1 for further discussion on the post-1979 period.

3.2. Anthropogenic Aerosol Influence Historical Trends in the Tropical Pacific SST Gradient Trends

Figure 1 motivates our research question for this section: *What forcing agents drive historical ensemble-mean SST gradient trends?* We explore the unique roles of anthropogenic aerosol, greenhouse gas and ozone forcing in driving the historical tropical Pacific SST gradient trends in climate models. The E:W trends for the 1950–2014 period are shown for each single-forcing experiment in Figure 2, together with observations and historical simulations previously shown in Figure 1. Trend maps for the ensemble-mean historical single forcing simulations are shown in S5–S8 of Supporting Information S1 for each model.

The natural forcings E:W trends are near-zero in each model, except MPI-ESM1-2-LR (−0.1 K per century). The ensemble-mean SST trend map for the natural forcings is not statistically significant in any region throughout the tropical Pacific for any of the four model (not shown).

The GHG forcing weakens the E:W gradient in each model, except MPI-ESM1-2-LR which has a near-zero ensemble-mean trend. In CanESM5 and HadGEM3-GC3.1-LL, the GHG induced SST warming trend pattern is statistically significant in all regions, except the Southern Hemisphere eastern subtropical SSTs, see Figures S5c and S7c in Supporting Information S1. In GISS-E2-1-G and MPI-ESM1-2-LR, the warming is not significant in the central-to-eastern tropical Pacific or the subtropical east Pacific in either hemisphere, see Figures S6c and S8c in Supporting Information S1). In all four models, the eastern subtropical warming due to GHGs is less pronounced. In the west Pacific, the SST warming is significant in each model. In the east Pacific, two of the models have significantly enhanced SST warming compared to the west—weakening the east-to-west gradient.

The AA forcing strengthens the SST gradient in the ensemble-mean in each model except GISS-E2-1-G. Despite different aerosol parameterizations in the *p1* and *p3* variants of GISS-E2-1-G, the spread in trends are similar and both have near-zero ensemble-mean trends. AA have broadly cooled the tropics in all four models, however, the trends in the east and central Pacific are not statistically significant, see Figures S5b–S8b in Supporting Information S1. While the MPI-ESM1-2-LR model has the largest ensemble-mean gradient trend, the SST trends are not significant throughout the tropical Pacific, see Figure S8b in Supporting Information S1.

The response of the tropical Pacific SSTs to O_3 are less robust across models. The ensemble-mean HadGEM3-GC3.1-LL trends are similar in magnitude for *hist-totalO3* and *hist-aer*. The HadGEM3-GC3.1-LL and *p1* variant of GISS-E2-1-G have similar *hist-totalO3* ensemble-mean trends. Unlike HadGEM3-GC3.1-LL, the GISS-E2-1-G model has the opposite trend response for *hist-totalO3* and *hist-aer*. The other two models have near-zero trends. The spatial pattern of SST trends is not significant throughout the tropical Pacific, see Figures S5d–S8d in Supporting Information S1. As such, we find no robust response of the SST trends to O_3 forcing in these models. We note that other models, such as CESM (Dong et al., 2025), have shown that O_3 impacts the tropical Pacific SST trend.

Compared to the 1950–2014 period, the models response during the shorter 1979–2014 period is similar in magnitude to the longer period for each of the single forcing experiments, see Figure S2 in Supporting Information S1. However, the observed trends in 1979–2014 are four-times larger. As such, the discrepancy between models and observations is much larger in the post-1979 period. While the HadGEM3-GC3.1-LL model strengthened due to AA forcing in 1950–2014, the trend is near-zero in the shorter 1979–2014 period.

Next we consider if the sum of the single-forcing ensemble-mean E:W trends are equal to the ensemble-mean trend in the all-forcings historical simulations. We do this separately for each model, see Table S4 in Supporting Information S1. HadGEM3-GC3.1-LL has an ensemble-mean historical trend of −0.076 K per century and the sum of the single forcing ensemble-means is −0.070 and for CanESM5 with 0.043 and 0.035, respectively. As such, these two models have historical SST gradients that can be explained by the linear combination of the GHG, AA and O_3 forcings. However, the other models have larger residuals, suggesting the linear combination of single-forcing agents does not fully explain the historical response.

Can the global-mean radiative forcing due to anthropogenic aerosols explain the inter-model differences in the tropical Pacific response? The radiative forcing is a measure of the energy imbalance due to a radiative perturbation. The Effective Radiative Forcing (ERF) is the Top-of-Atmosphere (TOA) flux difference between a perturbed and control simulation (Smith et al., 2020), where the perturbed forcing of interest in this study is AA forcing. The ERF due to anthropogenic aerosols (ERF_{AA}) is shown in Figure S9 of Supporting Information S1 for the CMIP6 historical models seen in Table 1. The ERF_{AA} values are taken from Table 3 of Griffiths et al. (2025)

10.1029/2025GL121248

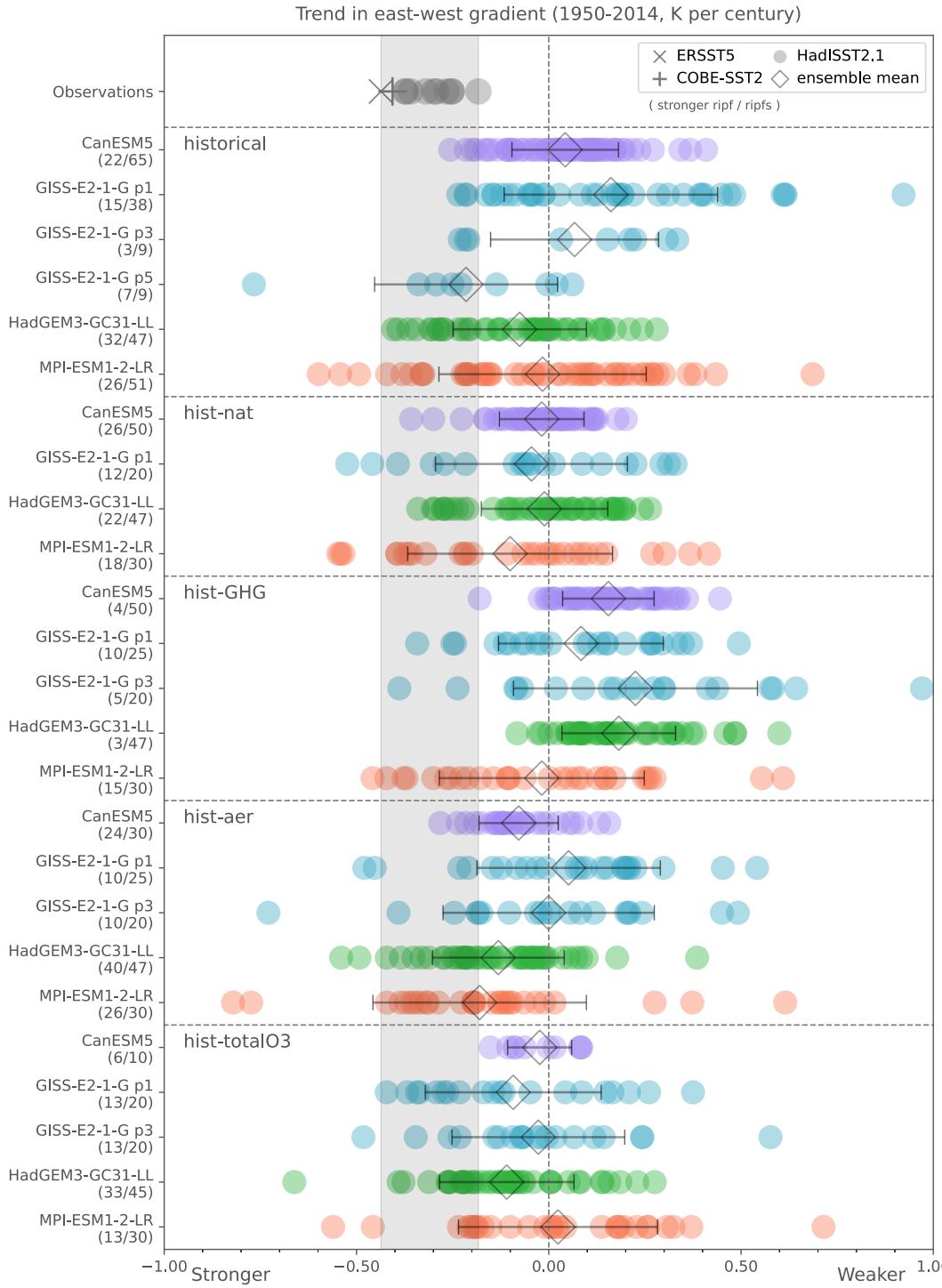

Figure 2. As in Figure 1 but for large-ensemble single-forcing simulations. The observations and historical simulations are the same as Figure 1. The numbers under the model names are the number of ensemble members that strengthen per ensemble size.

which used simulations from Radiative Forcing Model Intercomparison Project (RFMIP) (Pincus et al., 2016), see Supporting Information S1 for more information. The ERF_{AA} spans −0.59 to −1.32 W/m^2 for the historical CMIP6 models. The models ERF_{AA} are not correlated with the historical E:W metric trends in 1950–2014, with a correlation coefficient of 0.19 and broad scatter between the points.

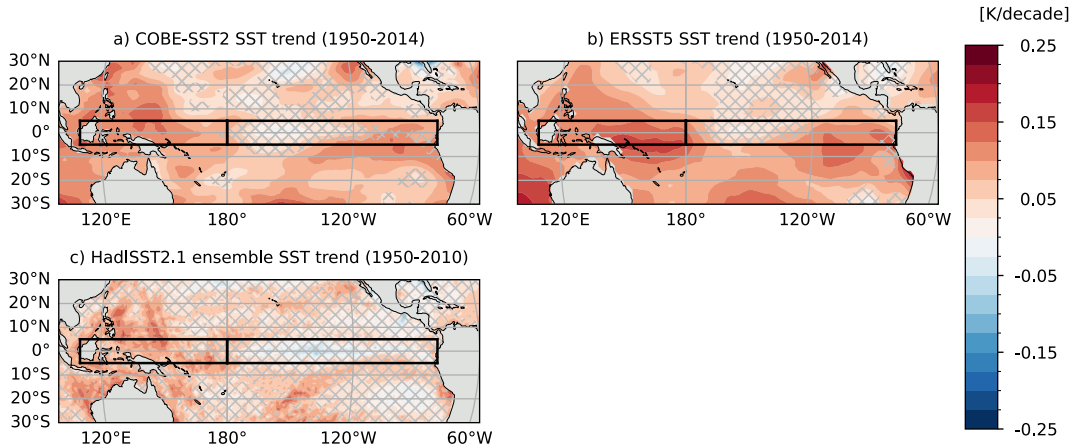

Figure 3. Tropical Pacific observed sea surface temperature trends (K/decade) for (a) COBE-SST2, (b) ERSST5, and (c) 10 member ensemble-mean of HadISST.2.1.0.0. The boxes are the east and west Pacific domains of the E:W ratio. Hatching is for trends that are not statistically significant at the 95% level. HadGEM3-GC3.1-LL *p*-values were combined using the Rüschendorf method (Choi & Kim, 2023), see Supporting Information S1 for more information. The resolution of the observed data sets are similar, see Table S1 in Supporting Information S1, but less smoothing is applied to the HadISST.2.1.0.0 data set which gives a false impression of resolution differences.

If the magnitude of global-mean anthropogenic aerosol forcing is not driving the tropical Pacific response, then perhaps it is the regional distribution of anthropogenic aerosols and the processes connecting it's radiative response to changes in the tropical Pacific. We test this by computing the TOA imbalance and shortwave (SW) TOA imbalance globally and over Asia, for the available CMIP6 models in Table 1. The trend in the E:W gradient SSTs are not significantly correlated (95% significance threshold) with the SW TOA imbalance due to anthropogenic aerosols in the global-mean, Asian, China-only (see Figure S10 in Supporting Information S1) and Indian-only (see Figure S11 in Supporting Information S1) regions for 1950–2014.

The choice of time period 1950–2014 strikes a delicate balance between maximizing signal-to-noise and averaging across two time periods with differing AA forcing trends. Indeed, the post-1980s period saw a reduction in AA forcing due to sulfur dioxide emission reductions across Europe and North America, in contrast to the earlier period where AA increased globally. However, during the same period, organic carbon and black carbon aerosol emissions have continued to increase. The experiments analyzed here do not allow us to identify which region or aerosol species are driving the response. Hopefully new experiments such as the Regional Aerosol Model Intercomparison Project (RAMIP, Wilcox et al. (2023)) may help answer these questions.

Further evidence to support the role of anthropogenic aerosols on the tropical Pacific gradient is shown in Figure S4 of Supporting Information S1, for HadGEM3-GC3.1-LL simulations where anthropogenic aerosols and their precursor emissions were scaled by factors between 0.2 and 1.5 their standard emissions, resulting in a wide range of realized AA forcing (Dittus et al., 2020). While the sample size of simulations per scaling (5) is smaller than those run for LESFMIP, the response across scalings generally supports the idea that anthropogenic aerosols are important for the tropical Pacific gradient trends.

3.3. Response in Simulations With Largest Strengthening Trends

Do ensemble members with the largest strengthening E:W trends have SST spatial patterns similar to observations? The observed equatorial SSTs have warmed in the west Pacific, but are not statistically significant in the central and eastern Pacific, see Figure 3. Trends may be non-significant due to weak trends, large natural variability, or a combination of the two. The trends in HadISST.2.1.0.0 are not significant in large areas of the tropical Pacific. These trend patterns are consistent with the literature (Seager et al., 2019). The east Pacific cooling seen in post-1979 trends (Heede & Fedorov, 2023; Watanabe et al., 2024) does not occur in the 1950–2014 period, contributing to the larger discrepancy between models and observations in 1979–2014.

The historical simulations with the five strongest E:W trends, that is, the five left-most historical realizations on Figure 2, are shown in Figure 4 for each model. The historical E:W strengthening occurs due to warming in the

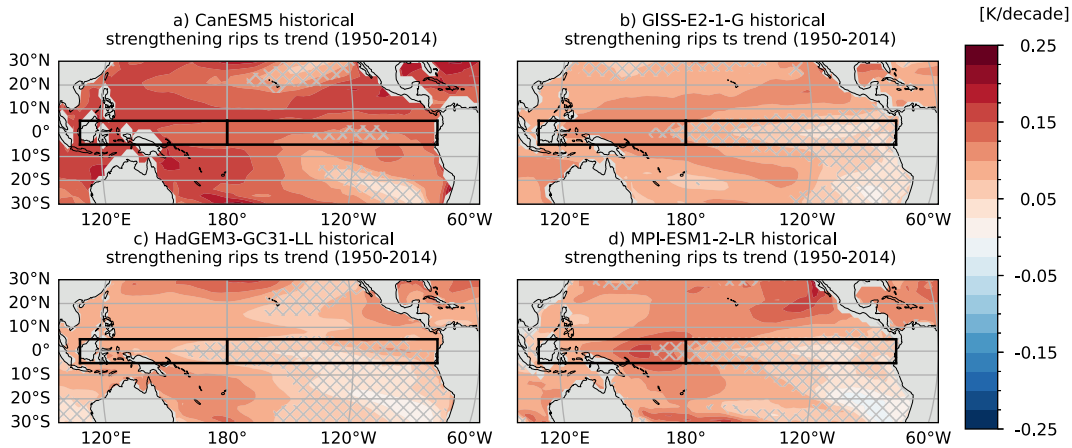

Figure 4. Tropical Pacific historical surface temperature *ts* trends for realizations with strongest east-to-west trends, that is, trend pattern corresponding to the five left-most historical simulations in Figure 1. Plotted are (a) CanESM5, (b) GISS-E2-1-G, (c) HadGEM3-GC31-LL and (d) MPI-ESM1-2-LR. Hatching is for trends that are not statistically significant at the 95% level.

western tropical Pacific, and, in general, weak or no change in the central or eastern tropical Pacific extending down to the subtropics. The historical warming in the west Pacific is primarily a balance between warming due to GHG forcing and cooling due to AA forcing, see Figures S13–S14 in Supporting Information S1. In the equatorial east Pacific, the warming due to GHG is statistically significant in two of the models, but the cooling due to AA in this region is only significant in one of the models. There is some suggestion of enhanced cooling of the equatorial central and eastern Pacific, however, the trends are not statistically significant. The trends in the ozone and natural forcing simulations are not significant throughout the tropical Pacific, see Figures S15 and S16 in Supporting Information S1.

3.4. Future Trends

Modeling the historical multi-decadal trends in the tropical Pacific remain problematic, with a compelling example being the 1979–2014 model-observations discrepancy in the tropical Pacific. Despite this, climate model simulations remain a key approach for exploring possible future climates. How will the tropical Pacific gradient change in the future? We consider two future emissions scenarios (SSP245 and SSP585), see Figure S3 in Supporting Information S1. We note that the ensemble-sizes vary considerable between the models, ranging from 4 to 50. The E:W ensemble-mean trend weakens in each model during the 2015–2100 period for both emissions scenarios, even for the models with historical strengthening trends. The trends are larger in the SSP585 simulations compared to SSP245. We interpret the weakening trends as a response to the increasing GHG forcing dominating over the AA forcing in the climate model future scenarios, especially in the SSP585 simulations. As the models can not capture the observed 1979–2014 cooling, it remains unclear if future projections in the tropical Pacific are reliable.

4. Conclusions

There remain three roadblocks to predicting future changes in tropical Pacific SSTs. What are the key processes driving observed tropical Pacific SST trends? How can we improve these key processes in climate models? What unique roles do internal variability and the forced response play in driving tropical Pacific SST trends? In this study we support progress in addressing these roadblocks, by exploring whether anthropogenic aerosols impact tropical Pacific gradient trends in historical simulations and how the trends will change in the future. In historical simulations during 1950–2014, only half of the models have ensemble mean tropical Pacific trends that strengthen like observations, and only one model is within the range of observations. The historical simulations with the largest E:W strengthening trends have spatial patterns of trends that are broadly consistent with observations in which the west Pacific is warming more than the central and east Pacific. The simulated historical tropical Pacific gradient change is primarily a balance between anthropogenic aerosols, which strengthen the trend, and greenhouse gas forcing, which weaken the trend. Neither the magnitude of the effective radiative forcing due to anthropogenic aerosols nor the trend in TOA imbalance due to anthropogenic aerosols can directly explain the

inter-model differences in the tropical Pacific response during 1950–2014. Likewise, regional trends in the TOA imbalances over Asia are not correlated with the E:W trends in 1950–2014. This suggests that processes connecting regional anthropogenic aerosol emissions to the tropical Pacific response are driving inter-model uncertainty in the historical simulations and further work in needed to understand the mechanisms. In future projections, all models have a weakening tropical Pacific gradient, irrespective of their historical response, which is likely a consequence of greenhouse gas forcing becoming dominant over anthropogenic aerosol forcing in the future. Our study highlights the need for further work to isolate how anthropogenic aerosols and their precursor emissions drive the physical processes which shape the tropical Pacific SST trends.

Conflict of Interest

The authors declare no conflicts of interest relevant to this study.

Availability Statement

Model data was downloaded from the Earth System Grid Federation (ESGF) grid. ERSST5 and COBE SST data sets were downloaded from https://downloads.psl.noaa.gov/Datasets/noaa.ersst.v5/sst.mnmean.nc and https://downloads.psl.noaa.gov/Datasets/COBE2/sst.mon.mean.nc. The HadISST.2.1.0.0 data set was downloaded from https://www.metoffice.gov.uk/hadobs/hadisst2/data/HadISST.2.1.0.0/index.html. See data citations in Table 1. The E:W metric trends generated in this study are provided in the zenodo repository 10.5281/zenodo.19334145 (Maher, 2026). This repository also contains the python scripts used to generate plots in this manuscript and perform the analysis.

Acknowledgments

We thank Tim Andrews, Harry Mutton, Laura Wilcox and Bjørn Samset for discussion on ERF and TOA energy imbalances. PM, RC and MC were funded by the NE/W005239/1 NERC Grant. AJD was funded by NERC Independent Research Fellowship NE/X017850/1. For the purpose of open access, the author has applied a Creative Commons Attribution (CC BY) license to any Author Accepted Manuscript version arising from this submission.

References

Andrews, T., Gregory, J. M., Paynter, D., Silvers, L. G., Zhou, C., Mauritsen, T., et al. (2018). Accounting for changing temperature patterns increases historical estimates of climate sensitivity. *Geophysical Research Letters*, *45*(16), 8490–8499. https://doi.org/10.1029/2018GL078887

Bethke, I., Wang, Y., Counillon, F., Keenlyside, N., Kimmritz, M., Fransner, F., et al. (2021). NorCPM1 and its contribution to CMIP6 DCPP. *Geoscientific Model Development*, *14*(11), 7073–7116. https://doi.org/10.5194/gmd-14-7073-2021

Bethke, I., Wang, Y., Counillon, F., Kimmritz, M., Fransner, F., Samuelsen, A., et al. (2019). NCC NorCPM1 model output prepared for CMIP6 CMIP historical. v20200724 [Dataset]. *Earth System Grid Federation*. https://doi.org/10.22033/ESGF/CMIP6.10894

Boucher, O., Denvil, S., Levavasseur, G., Cozic, A., Caubel, A., Foujols, M.-A., et al. (2018). IPSL IPSL-CM6A-LR model output prepared for CMIP6 CMIP historical. v20180803-v20211229 [Dataset]. *Earth System Grid Federation*. https://doi.org/10.22033/ESGF/CMIP6.5195

Boucher, O., Servonnat, J., Albright, A. L., Aumont, O., Balkanski, Y., Bastrikov, V., et al. (2020). Presentation and evaluation of the IPSL-CM6A-LR climate model. *Journal of Advances in Modeling Earth Systems*, *12*(7), e2019MS002010. https://doi.org/10.1029/2019MS002010

Byrne, H., Seager, R., & Smerdon, J. E. (2025). CMIP6 models cannot capture long-term forced changes in the tropical Pacific sea surface temperature gradient. *Nature Communications*, *17*(1), 142. https://doi.org/10.1038/s41467-025-66839-w

Byun, Y.-H. (2020). NIMS-KMA UKESM1.0-LL model output prepared for CMIP6 CMIP historical [Dataset]. Earth System Grid Federation. v20200205-v20210426. https://doi.org/10.22033/ESGF/CMIP6.8379

Choi, W., & Kim, I. (2023). Averaging p-values under exchangeability. *Statistics & Probability Letters*, *194*, 109748. https://doi.org/10.1016/j.spl.2022.109748

Clement, A. C., Burgman, R., & Norris, J. R. (2009). Observational and model evidence for positive low-level cloud feedback. *Science*, *325*(5939), 460–464. https://doi.org/10.1126/science.1171255

Clement, A. C., Seager, R., Cane, M. A., & Zebiak, S. E. (1996). An Ocean dynamical thermostat. *Journal of Climate*, *9*(9), 2190–2196. https://doi.org/10.1175/1520-0442(1996)009<2190:AODT>2.0.CO;2

Coats, S., & Karnauskas, K. B. (2017). Are simulated and observed twentieth Century Tropical Pacific Sea surface temperature trends significant relative to internal variability? *Geophysical Research Letters*, *44*(19), 9928–9937. https://doi.org/10.1002/2017GL074622

Dhame, S., Olonscheck, D., & Rugenstein, M. (2025). Higher-resolution climate models do not consistently reproduce the observed tropical pacific warming pattern. *Journal of Climate*, *38*(13), 3131–3149. https://doi.org/10.1175/JCLI-D-24-0248.1

Dittus, A. J., Hawkins, E., Wilcox, L. J., Sutton, R. T., Smith, C. J., Andrews, M. B., & Forster, P. M. (2020). Sensitivity of historical climate simulations to uncertain aerosol forcing. *Geophysical Research Letters*, *47*(13), e2019GL085806. https://doi.org/10.1029/2019GL085806

Dong, Y., Polvani, L. M., Hwang, Y.-T., & England, M. R. (2025). Stratospheric ozone depletion has contributed to the recent tropical la niña-like cooling pattern. *npj Climate and Atmospheric Science*, *8*(1), 150. https://doi.org/10.1038/s41612-025-01020-0

Döscher, R., Acosta, M., Alessandri, A., Anthoni, P., Arsouze, T., Bergman, T., et al. (2022). The EC-Earth3 Earth system model for the Coupled Model Intercomparison Project 6. *Geoscientific Model Development*, *15*(7), 2973–3020. https://doi.org/10.5194/gmd-15-2973-2022

EC-Earth Consortium. (2019). EC-Earth-Consortium EC-Earth3 model output prepared for CMIP6 CMIP historical [Dataset]. Earth System Grid Federation. v20200201-v20210604. https://doi.org/10.22033/ESGF/CMIP6.4700

Good, P., Chadwick, R., Holloway, C. E., Kennedy, J., Lowe, J. A., Roehrig, R., & Rushley, S. S. (2021). High sensitivity of tropical precipitation to local sea surface temperature. *Nature*, *589*(7842), 408–414. https://doi.org/10.1038/s41586-020-2887-3

Griffiths, P. T., Wilcox, L. J., Allen, R. J., Naik, V., O'Connor, F. M., Prather, M., et al. (2025). Opinion: The role of aerchemmip in advancing climate and air quality research. *Atmospheric Chemistry and Physics*, *25*(14), 8289–8328. https://doi.org/10.5194/acp-25-8289-2025

Günther, M., Kang, S., & Kaspi, Y. (2025). Heating the land cools the eastern and equatorial pacific. *Pre Print*. https://doi.org/10.21203/rs.3.rs-7189653/v1

Heede, U. K., & Fedorov, A. V. (2021). Eastern equatorial pacific warming delayed by aerosols and thermostat response to co2 increase. *Nature Climate Change*, *11*(8), 696–703. https://doi.org/10.1038/s41558-021-01101-x

Heede, U. K., & Fedorov, A. V. (2023). Colder eastern equatorial pacific and stronger walker circulation in the early 21st century: Separating the forced response to global warming from natural variability. *Geophysical Research Letters*, *50*(3), e2022GL101020. https://doi.org/10.1029/2022GL101020

Heede, U. K., Fedorov, A. V., & Burls, N. J. (2020). Time scales and mechanisms for the tropical pacific response to global warming: A tug of war between the ocean thermostat and weaker walker. *Journal of Climate*, *33*(14), 6101–6118. https://doi.org/10.1175/JCLI-D-19-0690.1

Hirahara, S., Ishii, M., & Fukuda, Y. (2014). Centennial-Scale Sea surface temperature analysis and its uncertainty. *Journal of Climate*, *27*(1), 57–75. https://doi.org/10.1175/JCLI-D-12-00837.1

Huang, B., Thorne, P. W., Banzon, V. F., Boyer, T., Chepurin, G., Lawrimore, J. H., et al. (2017a). Extended reconstructed Sea surface temperature, version 5 (ERSSTv5): Upgrades, validations, and intercomparisons. *Journal of Climate*, *30*(20), 8179–8205. https://doi.org/10.1175/JCLI-D-16-0836.1

Huang, B., Thorne, P. W., Banzon, V. F., Boyer, T., Chepurin, G., Lawrimore, J. H., et al. (2017b). *NOAA Extended Reconstructed Sea Surface Temperature (ERSST), version 5* [Dataset]. NOAA National Centers for Environmental Information. https://doi.org/10.7289/V5T72FNM

Hwang, Y.-T., Xie, S.-P., Chen, P.-J., Tseng, H.-Y., & Deser, C. (2024). Contribution of anthropogenic aerosols to persistent La Niña-like conditions in the early 21st century. *Proceedings of the National Academy of Sciences*, *121*(5), e2315124121. https://doi.org/10.1073/pnas.2315124121

Jiang, F., Seager, R., & Cane, M. A. (2024). A climate change signal in the tropical pacific emerges from decadal variability. *Nature Communications*, *15*(1), 8291. https://doi.org/10.1038/s41467-024-52731-6

Jiang, F., Seager, R., Cane, M. A., Karamperidou, C., & Brizuela, N. G. (2025). Subsurface cooling and sea surface temperature pattern formation over the equatorial pacific. *Journal of Geophysical Research: Oceans*, *130*(4), e2024JC022222. https://doi.org/10.1029/2024JC022222

Kang, S. M., Shin, Y., & Xie, S.-P. (2018). Extratropical forcing and tropical rainfall distribution: Energetics framework and ocean ekman advection. *npj Climate and Atmospheric Science*, *1*(1), 20172. https://doi.org/10.1038/s41612-017-0004-6

Kelley, M., Schmidt, G. A., Nazarenko, L. S., Bauer, S. E., Ruedy, R., Russell, G. L., et al. (2020). GISS-E2.1: Configurations and climatology. *Journal of Advances in Modeling Earth Systems*, *12*(8), e2019MS002025. https://doi.org/10.1029/2019MS002025

Kuhlbrodt, T., Jones, C. G., Sellar, A., Storkey, D., Blockley, E., Stringer, M., et al. (2018). The low-resolution version of HadGEM3 GC3.1: Development and evaluation for global climate. *Journal of Advances in Modeling Earth Systems*, *10*(11), 2865–2888. https://doi.org/10.1029/2018MS001370

Kuo, Y.-N., Kim, H., & Lehner, F. (2023). Anthropogenic aerosols contribute to the recent decline in precipitation over the u.s. southwest. *Geophysical Research Letters*, *50*(23), e2023GL105389. https://doi.org/10.1029/2023GL105389

Lee, S., L'Heureux, M., Wittenberg, A. T., Seager, R., O'Gorman, P. A., & Johnson, N. C. (2022). On the future zonal contrasts of equatorial pacific climate: Perspectives from observations, simulations, and theories. *npj Climate and Atmospheric Science*, *5*(1), 82. https://doi.org/10.1038/s41612-022-00301-2

Li, G., Xie, S.-P., Du, Y., & Luo, Y. (2016). Effects of excessive equatorial cold tongue bias on the projections of tropical pacific climate change. part i: The warming pattern in cmip5 multi-model ensemble. *Climate Dynamics*, *47*(12), 3817–3831. https://doi.org/10.1007/s00382-016-3043-5

Li, J. L. F., Xu, K.-M., Jiang, J. H., Lee, W.-L., Wang, L.-C., Yu, J.-Y., et al. (2020). An overview of cmip5 and cmip6 simulated cloud ice, radiation fields, surface wind stress, sea surface temperatures, and precipitation over tropical and subtropical oceans. *Journal of Geophysical Research: Atmospheres*, *125*(15), e2020JD032848. https://doi.org/10.1029/2020JD032848

Lin, J., & Qian, T. (2019). A new picture of the global impacts of el nino-southern oscillation. *Scientific Reports*, *9*(1), 17543. https://doi.org/10.1038/s41598-019-54090-5

Luongo, M. T., Xie, S.-P., Eisenman, I., Hwang, Y.-T., & Tseng, H.-Y. (2023). A pathway for northern hemisphere extratropical cooling to elicit a tropical response. *Geophysical Research Letters*, *50*(2), e2022GL100719. https://doi.org/10.1029/2022GL100719

Maher, P. (2026). Code and data for "Anthropogenic aerosols influence tropical Pacific sea surface temperature gradient trends". *Zenodo*. [Collection]. https://doi.org/10.5281/zenodo.19334145

Mauritsen, T., Bader, J., Becker, T., Behrens, J., Bittner, M., Brokopf, R., et al. (2019). Developments in the MPI-M Earth System Model version 1.2 (MPI-ESM1.2) and its Response to Increasing CO2. *Journal of Advances in Modeling Earth Systems*, *11*(4), 998–1038. https://doi.org/10.1029/2018MS001400

Milinski, S., Maher, N., & Olonscheck, D. (2020). How large does a large ensemble need to be? *Earth System Dynamics*, *11*(4), 885–901. https://doi.org/10.5194/esd-11-885-2020

Miller, R. L., Schmidt, G. A., Nazarenko, L. S., Bauer, S. E., Kelley, M., Ruedy, R., et al. (2021). CMIP6 Historical Simulations (1850–2014) with GISS-E2.1. *Journal of Advances in Modeling Earth Systems*, *13*(1), e2019MS002034. https://doi.org/10.1029/2019MS002034

MOHC. (2024). Hadley Centre Sea Ice and Sea Surface Temperature data set (HadISST.2.1.0.0) [Dataset]. *Data downloaded from*. Retrieved from https://www.metoffice.gov.uk/hadobs/hadisst2/data/HadISST.2.1.0.0/index.html

Mutton, H., Andrews, T., Hermanson, L., Seabrook, M., Smith, D. M., Ringer, M. A., et al. (2024). Feedbacks, pattern effects, and efficacies in a large ensemble of HadGEM3-GC3.1-LL historical simulations. *Journal of Geophysical Research: Atmospheres*, *129*(15), e2024JD041137. https://doi.org/10.1029/2024JD041137

NASA-GISS. (2018). NASA-GISS GISS-E2.1G model output prepared for CMIP6 CMIP historical [Dataset]. Earth System Grid Federation. v20180827-v20190905. https://doi.org/10.22033/ESGF/CMIP6.7127

Olonscheck, D., Rugenstein, M., & Marotzke, J. (2020). Broad consistency between observed and simulated trends in Sea surface temperature patterns. *Geophysical Research Letters*, *47*(10), e2019GL086773. https://doi.org/10.1029/2019GL086773

Pincus, R., Forster, P. M., & Stevens, B. (2016). The Radiative Forcing Model Intercomparison Project (RFMIP): Experimental protocol for CMIP6. *Geoscientific Model Development*, *9*(9), 3447–3460. https://doi.org/10.5194/gmd-9-3447-2016

PSL. (2023). COBE-SST 2 data provided by the NOAA PSL [Dataset]. Retrieved from https://psl.noaa.gov

Rayner, N. A., Parker, D. E., Horton, E. B., Folland, C. K., Alexander, L. V., Rowell, D. P., et al. (2003). Global analyses of sea surface temperature, sea ice, and night marine air temperature since the late nineteenth century [Dataset]. *Journal of Geophysical Research*, *108*(D14). https://doi.org/10.1029/2002JD002670

Ridley, J., Menary, M., Kuhlbrodt, T., Andrews, M., & Andrews, T. (2019). MOHC HadGEM3-GC31-LL model output prepared for CMIP6 CMIP historical [Dataset]. Earth System Grid Federation. v20190624-v20230711. https://doi.org/10.22033/ESGF/CMIP6.6109

Ridley, J. K., Blockley, E. W., & Jones, G. S. (2022). A change in climate State during a pre-industrial simulation of the CMIP6 model HadGEM3 driven by deep Ocean drift. *Geophysical Research Letters*, *49*(6), e2021GL097171. https://doi.org/10.1029/2021GL097171

Rugenstein, M., Dhame, S., Olonscheck, D., Wills, R. J., Watanabe, M., & Seager, R. (2023). Connecting the sst pattern problem and the hot model problem. *Geophysical Research Letters*, *50*(22), e2023GL105488. https://doi.org/10.1029/2023GL105488

Seager, R., Cane, M., Henderson, N., Lee, D.-E., Abernathey, R., & Zhang, H. (2019). Strengthening tropical Pacific zonal sea surface temperature gradient consistent with rising greenhouse gases. *Nature Climate Change*, *9*(7), 517–522. https://doi.org/10.1038/s41558-019-0505-x

Sellar, A. A., Jones, C. G., Mulcahy, J. P., Tang, Y., Yool, A., Wiltshire, A., et al. (2019). UKESM1: Description and evaluation of the U.K. Earth System model. *Journal of Advances in Modeling Earth Systems*, *11*(12), 4513–4558. https://doi.org/10.1029/2019MS001739

Simpson, I. R., Shaw, T. A., Ceppi, P., Clement, A. C., Fischer, E., Grise, K. M., et al. (2025). Confronting earth system model trends with observations. *Science Advances*, *11*(11), eadt8035. https://doi.org/10.1126/sciadv.adt8035

Smith, C. J., Kramer, R. J., Myhre, G., Alterskjær, K., Collins, W., Sima, A., et al. (2020). Effective radiative forcing and adjustments in CMIP6 models. *Atmospheric Chemistry and Physics*, *20*(16), 9591–9618. https://doi.org/10.5194/acp-20-9591-2020

Smith, D. M., Gillett, N. P., Simpson, I. R., Athanasiadis, P. J., Baehr, J., Bethke, I., et al. (2022). Attribution of multi-annual to decadal changes in the climate system: The Large Ensemble Single Forcing Model Intercomparison Project (LESFMIP). *Frontiers in Climate*, *4*, 955414. https://doi.org/10.3389/fclim.2022.955414

Sobel, A. H., Lee, C.-Y., Bowen, S. G., Camargo, S. J., Cane, M. A., Clement, A., et al. (2023). Near-term tropical cyclone risk and coupled earth system model biases. *Proceedings of the National Academy of Sciences*, *120*(33), e2209631120. https://doi.org/10.1073/pnas.2209631120

Sung, H. M., Kim, J., Shim, S., Seo, J.-b., Kwon, S.-H., Sun, M.-A., et al. (2021). Climate change projection in the twenty-first century simulated by NIMS-KMA CMIP6 model based on new GHGs concentration pathways. *Asia-Pacific Journal of Atmospheric Sciences*, *57*(4), 851–862. https://doi.org/10.1007/s13143-021-00225-6

Swart, N. C., Cole, J. N. S., Kharin, V. V., Lazare, M., Scinocca, J. F., Gillett, N. P., et al. (2019a). The Canadian Earth System Model version 5 (CanESM5.0.3). *Geoscientific Model Development*, *12*(11), 4823–4873. https://doi.org/10.5194/gmd-12-4823-2019

Swart, N. C., Cole, J. N. S., Kharin, V. V., Lazare, M., Scinocca, J. F., Gillett, N. P., et al. (2019b). CCCma CanESM5 model output prepared for CMIP6 CMIP historical [Dataset]. *Earth System Grid Federation*. https://doi.org/10.22033/ESGF/CMIP6.3610

Tang, Y., Rumbold, S., Ellis, R., Kelley, D., Mulcahy, J., Sellar, A., et al. (2019). MOHC UKESM1.0-LL model output prepared for CMIP6 CMIP historical [Dataset]. *Earth System Grid Federation*. v20190406-20191213. https://doi.org/10.22033/ESGF/CMIP6.6113

Tatebe, H., Ogura, T., Nitta, T., Komuro, Y., Ogochi, K., Takemura, T., et al. (2019). Description and basic evaluation of simulated mean state, internal variability, and climate sensitivity in MIROC6. *Geoscientific Model Development*, *12*(7), 2727–2765. https://doi.org/10.5194/gmd-12-2727-2019

Tatebe, H., & Watanabe, M. (2018). MIROC MIROC6 model output prepared for CMIP6 CMIP historical [Dataset]. Earth System Grid Federation. v20181212-v20200519. https://doi.org/10.22033/ESGF/CMIP6.5603

Titchner, H. A., & Rayner, N. A. (2014). The Met Office Hadley Centre sea ice and sea surface temperature data set, version 2: 1. Sea ice concentrations. *Journal of Geophysical Research: Atmospheres*, *119*(6), 2864–2889. https://doi.org/10.1002/2013JD020316

Verma, T., Saravanan, R., Chang, P., & Mahajan, S. (2019). Tropical pacific ocean dynamical response to short-term sulfate aerosol forcing. *Journal of Climate*, *32*(23), 8205–8221. https://doi.org/10.1175/JCLI-D-19-0050.1

Voldoire, A. (2018). CMIP6 simulations of the CNRM-CERFACS based on CNRM-CM6-1 model for CMIP experiment historical. v20181126-v20200529 [Dataset]. *Earth System Grid Federation*. https://doi.org/10.22033/ESGF/CMIP6.4066

Voldoire, A., Saint-Martin, D., Sénési, S., Decharme, B., Alias, A., Chevallier, M., et al. (2019). Evaluation of CMIP6 DECK experiments with CNRM-CM6-1. *Journal of Advances in Modeling Earth Systems*, *11*(7), 2177–2213. https://doi.org/10.1029/2019MS001683

Watanabe, M., Dufresne, J.-L., Kosaka, Y., Mauritsen, T., & Tatebe, H. (2021). Enhanced warming constrained by past trends in equatorial Pacific sea surface temperature gradient. *Nature Climate Change*, *11*(1), 33–37. https://doi.org/10.1038/s41558-020-00933-3

Watanabe, M., Kang, S. M., Collins, M., Hwang, Y.-T., McGregor, S., & Stuecker, M. F. (2024). Possible shift in controls of the tropical Pacific surface warming pattern. *Nature*, *630*(8016), 315–324. https://doi.org/10.1038/s41586-024-07452-7

Wieners, K.-H., Giorgetta, M., Jungclaus, J., Reick, C., Esch, M., Bittner, M., et al. (2019). MPI-M MPI-ESM1.2-LR model output prepared for CMIP6 CMIP historical [Dataset]. *Earth System Grid Federation*. https://doi.org/10.22033/ESGF/CMIP6.6595

Wilcox, L. J., Allen, R. J., Samset, B. H., Bollasina, M. A., Griffiths, P. T., Keeble, J., et al. (2023). The regional aerosol model intercomparison project (ramip). *Geoscientific Model Development*, *16*(15), 4451–4479. https://doi.org/10.5194/gmd-16-4451-2023

Wills, R. C. J., Dong, Y., Proistosecu, C., Armour, K. C., & Battisti, D. S. (2022). Systematic climate model biases in the large-scale patterns of recent sea-surface temperature and sea-level pressure change. *Geophysical Research Letters*, *49*(17), e2022GL100011. https://doi.org/10.1029/2022GL100011

Ying, J., Collins, M., Cai, W., Timmermann, A., Huang, P., Chen, D., & Stein, K. (2022). Emergence of climate change in the tropical pacific. *Nature Climate Change*, *12*(4), 356–364. https://doi.org/10.1038/s41558-022-01301-z

Ying, J., Huang, P., & Huang, R. (2016). Evaluating the formation mechanisms of the equatorial pacific sst warming pattern in cmip5 models. *Advances in Atmospheric Sciences*, *33*(4), 433–441. https://doi.org/10.1007/s00376-015-5184-6

Ziehn, T., Chamberlain, M., Lenton, A., Law, R., Bodman, R., Dix, M., et al. (2019). CSIRO ACCESS-ESM1.5 model output prepared for CMIP6 CMIP historical v20191115-v20210525 [Dataset]. *Earth System Grid Federation*. https://doi.org/10.22033/ESGF/CMIP6.4272

Ziehn, T., Chamberlain, M. A., Law, R. M., Lenton, A., Bodman, R. W., Dix, M., et al. (2020). The Australian Earth System model: ACCESS-ESM1.5. *JSHESS*, *70*(1), 193–214. https://doi.org/10.1071/es19035